Transport of Fragile X Mental Retardation Protein via Granules in Neurites of PC12 Cells

Yolanda De Diego Otero,[1]† Lies-Anne Severijnen,[1] Gert van Cappellen,[2] Mariëtte Schrier,[1] Ben Oostra,[1] and Rob Willemsen[1]*

CBG Department of Clinical Genetics[1] and Department of Endocrinology and Reproduction,[2] Erasmus University, Rotterdam, The Netherlands

Lack of fragile X mental retardation protein (FMRP) causes fragile X syndrome, a common form of inherited mental retardation. FMRP is an RNA binding protein thought to be involved in translation efficiency and/or trafficking of certain mRNAs. Recently, a subset of mRNAs to which FMRP binds with high affinity has been identified. These FMRP-associated mRNAs contain an intramolecular G-quartet structure. In neurons, dendritic mRNAs are involved in local synthesis of proteins in response to synaptic activity, and this represents a mechanism for synaptic plasticity. To determine the role of FMRP in dendritic mRNA transport, we have generated a stably FMR1-enhanced green fluorescent protein (EGFP)-transfected PC12 cell line with an inducible expression system (Tet-On) for regulated expression of the FMRP-GFP fusion protein. After doxy-cycline induction, FMRP-GFP was localized in granules in the neurites of PC12 cells. By using time-lapse microscopy, the trafficking of FMRP-GFP granules into the neurites of living PC12 cells was demonstrated. Motile FMRP-GFP granules displayed two types of movements: oscillatory (bidirectional) and unidirectional anterograde. The average velocity of the granules was 0.19 μm/s with a maximum speed of 0.71 μm/s. In addition, we showed that the movement of FMRP-GFP labeled granules into the neurites was microtubule dependent. Colocalization studies further showed that the FMRP-GFP labeled granules also contained RNA, ribosomal subunits, kinesin heavy chain, and FXR1P molecules. This report is the first example of trafficking of RNA-containing granules with FMRP as a core constituent in living PC12 cells.

Fragile X syndrome is one of the most prevalent causes of inheritable mental retardation, with a frequency of 1:4,000 males (26). This X-linked disorder is caused by the absence of the fragile X mental retardation protein (FMRP). FMRP expression is widespread with abundant expression in neurons and trafficking to dendrites in particular and with testicular expression in spermatogonia (3, 14, 15, 38, 43). The association of FMRP with ribosomes is mRNA dependent via ribonucleoprotein (RNP) particles, which contain several other proteins including the fragile X (structurally)-related proteins FXR1P and FXR2P (10). Microscopic analysis of autopsy material from fragile X patients and brain pathology studies of Fmr1-knockout mice have indicated dendritic spines abnormal in size and shape, and a function in maturation of spines has been attributed to FMRP (11, 19).

FMRP contains RNA-binding sequence motifs, including two KH domains and an RGG box (2, 34). The precise physiological function of FMRP is still not defined; however, a role in transport and/or translational efficiency of mRNAs has been suggested elsewhere (27, 28). Recently, there has been identified a subset of mRNAs containing a G quartet that is a potential target for FMRP, including those for important neuronal proteins like microtubule-associated protein MAP1B and semaphorin (6, 13). It has been suggested that the absence of FMRP in neurons results in misregulation or mistrafficking of a subset of mRNAs and that this is the basis of the mental retardation in fragile X syndrome.

Interestingly, recent evidence shows that mRNA transport-translation in dendrites plays an important role in neuronal processes, including synaptic plasticity, which is essential for memory storage and learning processes (21). Most dendritic polyribosomes are located within or at the base of spines, and it has been hypothesized that local protein synthesis at the synapse may be an important aspect of proper synaptogenesis (35). The presence of the protein machinery, postsynaptically, allows neurons to rapidly respond to signals at particular synapses through local translation of (specific) mRNAs. For this purpose, efficient transport of specific mRNAs, via mRNP particles, has to be established to this cellular location followed by efficient translation of mRNAs in the vicinity of the synapse.

The dynamics of the transport of mRNP particles in neurons have been studied by different experimental approaches, and a supramolecular complex containing mRNAs, translational factors, and ribosomal subunits has been identified (4). The migration of mRNP particles over long distances within the dendrites toward the growth cone is established by movement along microtubules via a mechanism involving cytoplasmic kinesin, a plus-end-directed microtubule motor protein (8, 24, 25, 39). On the other hand the migration of mRNP particles over shorter distances may require microfilaments, such as actin filaments for the transport of β-actin mRNAs in fibroblasts (37).

Since FMRP in neurons may be involved in local dendritic protein synthesis, related to synaptic function and plasticity, it

---

* Corresponding author. Mailing address: Department of Clinical Genetics, Erasmus University, P.O. Box 1738, 3000 DR Rotterdam, The Netherlands. Phone: (31) 10-4087152. Fax: (31) 10-4089489. E-mail: willemsen@ch1.fgg.eur.nl.

† Present address: Carlos Haya Hospital Research Laboratory, Malaga, Spain.

is important to identify the subset of target mRNAs and understand how FMRP functions in their delivery into the dendrites. In the present study we visualized FMRP in vivo in a PC12 cell line stably transfected with a human FMR1-enhanced green fluorescent protein fusion (FMR1-EGFP) gene as a first step to study the role of FMRP-GFP-containing granules in dendritic mRNA transport and translation.

MATERIALS AND METHODS

Cell culture, expression vectors, and transfection. Rat pheochromocytoma cells (PC12) were used with a Tet-On gene expression system because this cell system permits tightly regulated expression of the FMR1 gene in response to doxycycline (DOX; doxycycline hydrochloride; Sigma D9891; 1 μg/ml). PC12 Tet-On cells were obtained from Clontech and grown as specified by the manufacturer. Briefly, cells were cultured in Dulbecco modified Eagle medium (DMEM) supplemented with 10% horse serum, 5% fetal bovine serum, 125 μg of hygromycin/ml, 100 μg of penicillin-streptomycin/ml, and 100 μg of G418/ml in a 10% CO_2 incubator at 37°C. PC12 cells were differentiated into a neuronal phenotype on collagen-coated coverslips in medium supplemented with 100 ng of nerve growth factor (NGF-7S; Sigma)/ml for 72 h (DMEM, G418, hygromycin, 0.75% horse serum, 0.25% fetal bovine serum).

The cloning of the expression plasmids for the human FMRP-GFP fusion protein (pFMRP-EGFP) was described by Castren et al. (9). The pFMRP-EGFP construct was cloned into the pTRE response plasmid (Clontech) to generate a double stable transfected Tet-On cell line, by the Lipofectamine procedure (30 μl of Lipofectamine from GibcoBRL and 20 μg of plasmid DNA). The pHyg resistance vector was used in the cotransfection as a selection marker. Transfected cells were cultured in medium containing hygromycin (0.125 mg/ml; GibcoBRL) and DOX (1 μg/ml), and subsequently individual double stable cell colonies were tested and further selected for the presence of the FMRP-GFP fusion protein by fluorescence microscopy. Several cell lines ($n = 11$) were selected on the basis of both the presence of FMRP-GFP fusion protein after DOX treatment and the absence of the FMRP-GFP fusion protein without DOX treatment (leakage) and further investigated by Western blotting and immunocytochemistry.

For primary cultures of mouse (wild-type [wt]) hippocampal neurons, hippocampi were dissected from E19 old mouse brains and prepared and cultured as described before (38).

Antibodies and reagents. The following antibodies were used: monoclonal antibody to human FMRP (clone 1C3; 1:800) (14), monoclonal anti-GFP antibody (1:2,000; Roche USA no. 1814460), monoclonal anti-FXR1P (3FX; 1:500) (20), monoclonal anti-tyrosine-tubulin (1:100; clone TUB-1A2; Sigma), human anti-ribosomal P antigen (1:100; P0; Immunovision), and monoclonal anti-kinesin heavy chains (1:100; clone IBII; Sigma). Texas red-labeled phallotoxins were used to visualize F-actin (1:50; T-7471; Molecular Probes). As secondary antibodies we used swine anti-rabbit immunoglobulin (Ig) conjugated with horseradish peroxidase (HRP; 1:100; P0217; DAKO), goat anti-human Ig conjugated with tetramethyl rhodamine isocyanate (TRITC; 1:100; T-5903; Sigma), and rabbit anti-mouse Ig conjugated with HRP (1:100; P0260; DAKO). We used 1 μM ethidium bromide (EtBr; Fluka) in phosphate-buffered saline (PBS) to fluorescently label total cellular RNA according to the method of Tang et al. (39). Under these experimental conditions, the EtBr signal is sensitive to RNase treatment but not for DNase treatment, indicating specificity for RNA localization. Unfortunately, the fluorescent dye SYTO14 could not be used to label cellular RNA because the emitted light of SYTO14 overlapped with GFP fluorescence.

All drug treatments were carried out in DMEM (complete) at 37°C. To block mRNA translation, cells were pretreated with DOX for 30 min followed by treatment with cycloheximide (30 μg/ml; Sigma) for another 2 h. This concentration of cycloheximide results in a total block of protein synthesis, which was demonstrated by treatment of PC12/FMR7 cells with DOX and cycloheximide simultaneously for 6 h (data not shown). To disrupt microfilaments, cells were pretreated for 30 min with DOX followed by treatment with both DOX and cytochalasin D (5 μg/ml; Sigma) for another 2 h before fixation. Depolymerization of microtubules was accomplished by pretreatment of cells with DOX for 30 min followed by treatment with both DOX and nocodazole (10 μM; Sigma) for another 2 h before fixation.

Western blotting and immunocytochemistry. PC12 Tet-On cells and 11 selected PC12 Tet-On cell lines stably transfected with pFMRP-EGFP (designated PC12/FMR1 to PC12/FMR11) were grown with and without the presence of
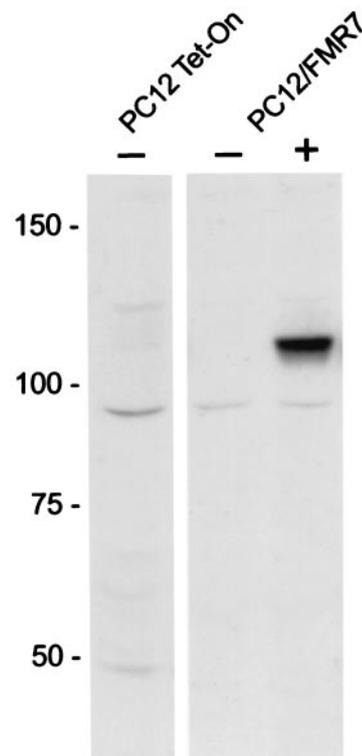

FIG. 1. Western blotting with specific antibodies to GFP of PC12 Tet-On (control) and stable transfected PC12/FMR7 cells with (+) and without (−) DOX induction. PC12/FMR7 cells show the presence of a band of approximately 110 kDa after DOX induction with the anti-GFP antibody, which is the expected size for the full-length FMRP-GFP fusion protein (80 plus 27 kDa). In contrast, PC12/FMR7 cells without DOX induction are devoid of the 110-kDa band, representing the absence of nonspecific induction (leakage). In PC12 Tet-On cells no detection of the 110-kDa band was observed. Numbers at left show molecular masses in kilodaltons.

DOX. Cells were harvested after 24 h, and lysates from the different cell lines were run on a 10% gel and blotted onto nitrocellulose. Immunodetection of the FMRP-GFP fusion protein was performed with monospecific antibodies against GFP followed by an incubation with secondary antibodies coupled to peroxidase, allowing detection by the chemiluminescence method (ECL kit; Amersham).

Cellular FMRP-GFP distribution was studied by both direct immunofluorescence and the indirect immunoperoxidase technique. Cells were cultured on collagen-coated coverslips and treated with NGF for 72 h followed by treatment with both DOX and NGF for times varying from 1 to 72 h. For direct visualization of GFP by immunofluorescence, cells were fixed with 95% ethanol for 30 min at room temperature (RT). Wash steps were carried out with 0.1 M PBS, and coverslips were mounted with Vectashield mounting medium. In the colocalization studies, cells were incubated with primary antibodies against different markers (see above for antibodies) for 1 h at RT followed by a 45-min incubation with TRITC-conjugated secondary antibodies. Cells were examined with a Leitz fluorescence microscope with a 63× objective, standard fluorescein isothiocyanate and TRITC filters, a 100-W HBO mercury light source, and a Sony DXC-95OP 3CCD color video camera.

The endogenous FMRP expression in both PC12 cells and primary mouse (wt) hippocampal neurons was studied by an indirect immunofluorescence technique with monoclonal antibodies to FMRP (14). For indirect immunoperoxidase labeling, cells were fixed in 3% paraformaldehyde for 10 min at RT, followed by a permeabilization step in 100% methanol for 20 min at RT. Endogenous peroxidase activity was blocked by a 30-min preincubation in 0.1 M PBS, containing 0.6% H_2O_2 and 0.12% sodium azide, and nonspecific binding sites were blocked by incubation with 0.1 M PBS containing 0.5% bovine serum albumin and 0.15% glycine for 10 min at RT. Subsequently, cells were incubated with primary antibodies for 1 h at RT followed by a 45-min incubation with an
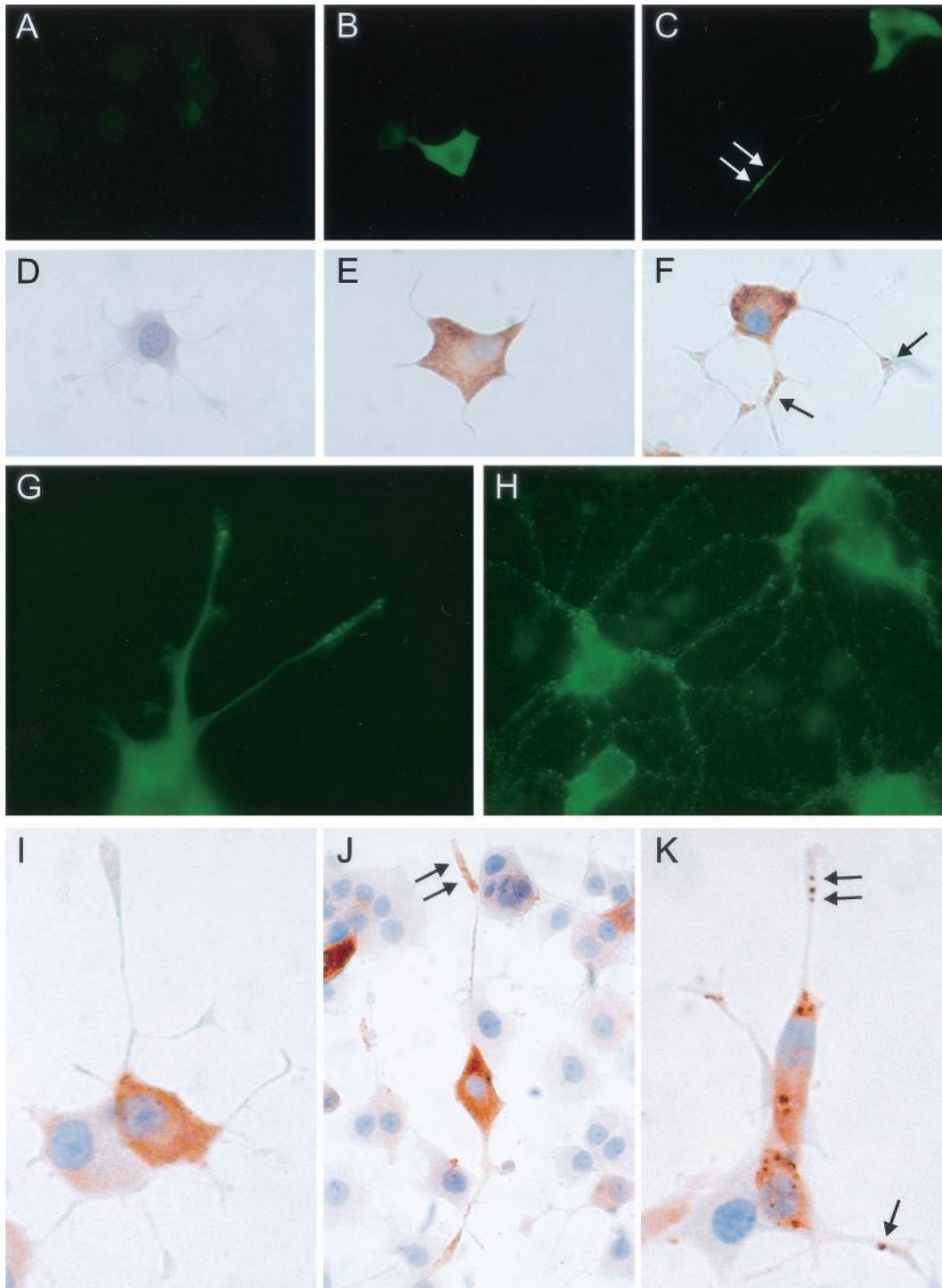
FIG. 2. Light microscopic appearance of movement of FMRP-GFP granules into neurites of PC12/FMR7 cells after DOX induction. The FMRP-GFP fusion protein was visualized either directly by immunofluorescence of the GFP molecules (A to C) or by an indirect immunoperoxidase technique with specific antibodies to GFP (D to F). Without DOX induction (A and D; time zero) no reaction product could be visualized. After 30 min of DOX induction FMRP-GFP fusion protein was present solely in the cell body (B and E). Exposure of the cells to DOX for 2 h revealed a strong labeling in the cell body and a punctate labeling pattern in the neurites (C and F, arrows). Especially in the bright-field images from the immunoperoxidase-incubated cells, swellings along the neurite with high concentrations of granules could be observed (F, arrows). Panels G and H illustrate the endogenous FMRP expression in untransfected PC12 cells and primary mouse hippocampal neurons, respectively. PC12/FMR7 cells were cultured for 30 min in the presence of DOX (I); subsequently cells were cultured for another 2 h in medium containing DOX with (J) and without (K) the presence of cycloheximide. In the presence of cycloheximide the FMRP-GFP fusion protein is still able to reach the neurites (K, arrows). Magnifications: A to C, ×720; D to F, ×960; G, ×1,200; H, ×960; I and K, ×1,440; J, ×800.
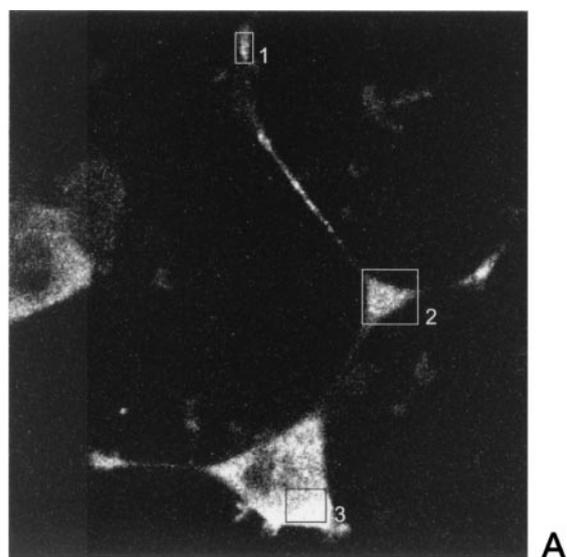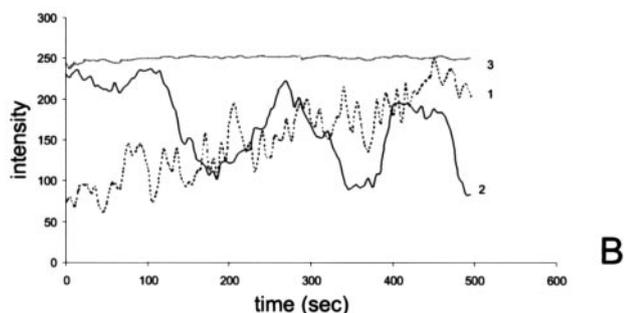
FIG. 3. (A) Figure corresponding to time-lapse series 1 (available online); individual FMRP-GFP labeled granules were observed by time-lapse microscopy. The time-lapse series shows the movement of green fluorescent granules in PC12/FMR7 cells after DOX induction (2 h) in a time-lapse study of frames every 5 s for 500 s. Note the movement of fluorescent granules between the swelling along the neurite (square 2) and the growth cone (rectangle 1). (B) Quantification of the emission intensities over time (500 s). The overall emission intensity in the cell body (square 3) remains the same over time, whereas the emission intensity within the swelling (square 2) follows a cycle every 3 min. The emission profile of the growth cone shows a gradual increase of intensity during the recorded time (rectangle 1).

HRP-conjugated secondary antibody. Enzymatic detection of antigen-antibody complexes was achieved by incubation in substrate solution containing H_2O_2 and 3′,3′-diaminobenzidine tetrahydrochloride (DAB; DAKO). Finally, cells were counterstained with hematoxylin and mounted with Aquamount (Gurr; BDH). Labeling specificity was verified by incubations without primary or secondary antibody. In both cases, background labeling was negligible.

Confocal microscopy. Time-lapse microscopy recording at physiological temperature (37°C) of living stable transfected PC12 cells (PC12/FMR7) grown on coverslips was performed in the presence of both NGF and DOX with a Zeiss LSM510NLO microscope. The following setup was used: excitation, 488 nm; 0.5% acoustic optical tunable filter; main dichroic beam splitter (HFT); emission filter, BP 500 to 550. Simultaneously with the fluorescent image a Nomarski image was made.

For quantification, stable transfected cells were chosen by green fluorescence and images were recorded and evaluated for the intensity of fluorescence at different areas within the cell (cell body, neurite, and growth cone) with the Zeiss advanced imaging microscopy software package. To calculate the average speed (micrometers per second) of individual fluorescent granules, the distance traveled from 25 different granules was measured during two or more consecutive time-lapse frames (average number of frames, 12) with the Zeiss advanced imaging microscopy software package and divided by time.

RESULTS

After DOX-induced expression, 11 stable transfected Tet-On cell lines with pFMRP-EGFP were selected by screening for the presence of GFP by immunofluorescence microscopy. From those 11 cell lines we have chosen the PC12/FMR7 cell line by two criteria as the most suitable cell line for further studies: first, FMRP-GFP expression levels after DOX induction were not too high, and second, without DOX FMRP-GFP expression was absent. In particular, the moderate expression level after DOX induction is important because high FMRP expression levels have been shown previously to be toxic for cells after transfection (10). Figure 1 shows a Western blot and illustrates the presence of FMRP-GFP after DOX induction and the absence of FMRP-GFP without DOX induction in the PC12/FMR7 cell line. The observed molecular mass of approximately 110 kDa is in line with what was expected, that is, 80 kDa for FMRP and 27 kDa for GFP. As a negative control, the original PC12 Tet-On cell line that was used to generate the stable transfectant cell line was included.

Further characterization of the PC12/FMR7 cell line was performed to study the pattern of expression and cellular lo-
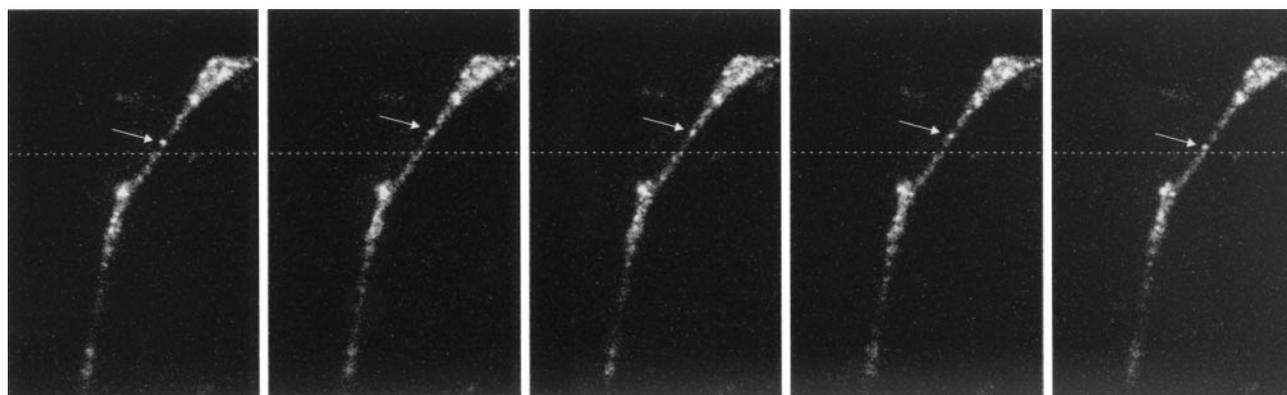

FIG. 4. Figure corresponding to time-lapse series 2 (available online); individual time-lapse frames were more highly integrated than those of time-lapse series 1 (every second for 300 s). We have focused on the movement of granules between the swelling along the neurite and the growth cone already described for time-lapse series 1. A selection of consecutive time-lapse frames illustrates the bidirectional movement (arrows) of an individual granule. The bidirectional movement of this particular granule switched later in the time-lapse series to a distal unidirectional movement followed by appearance in the growth cone.
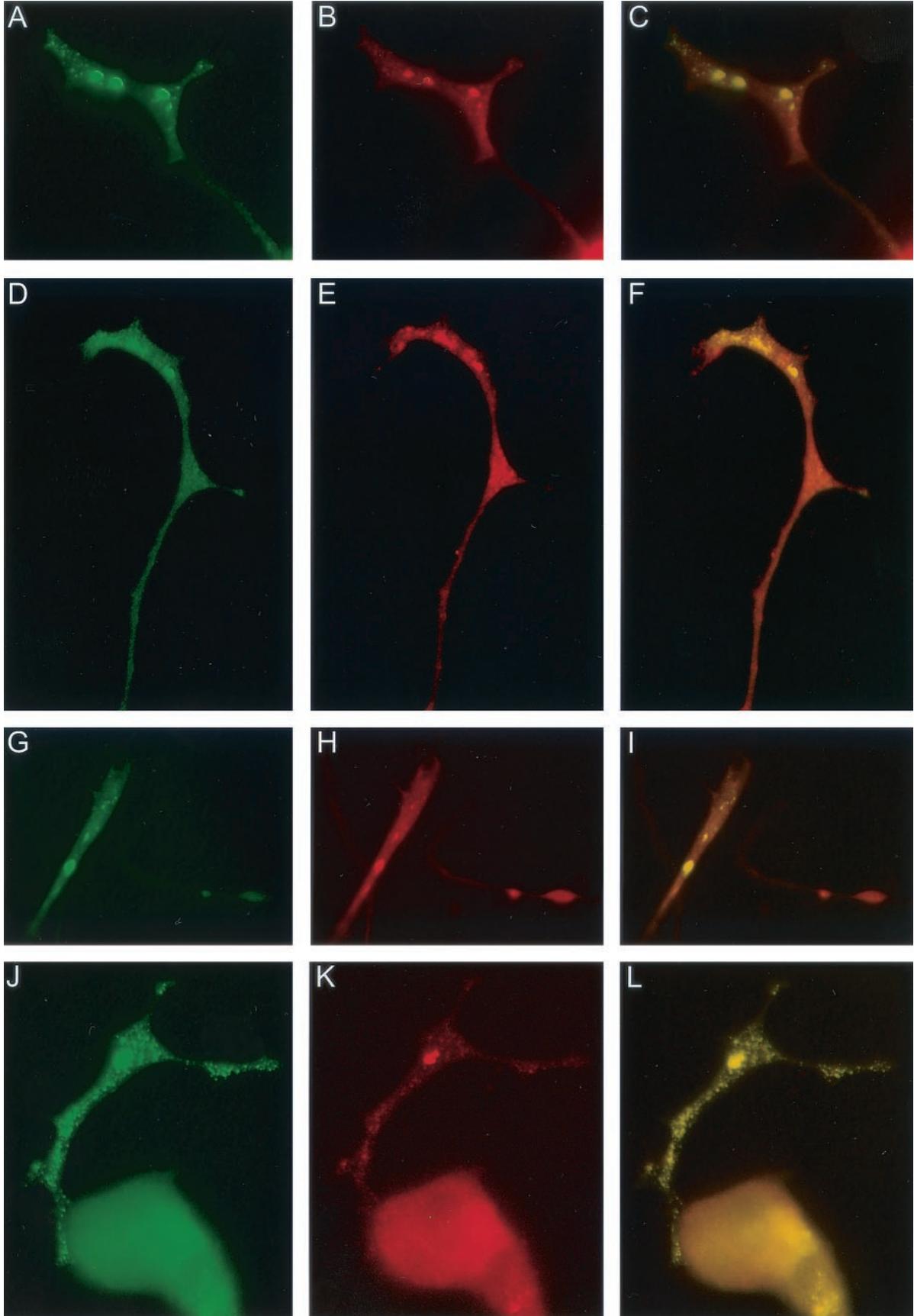
calization of FMRP-GFP after both NGF exposure and DOX induction. In a time series experiment FMRP-GFP was visualized either by direct visualization of green fluorescence (Fig. 2A to C) or by the indirect immunoperoxidase technique with specific antibodies to GFP (Fig. 2D to F). At time zero (with NGF exposure and without DOX induction) FMRP-GFP was absent in PC12/FMR7 cells (Fig. 2A and D). At 30 min after DOX induction FMRP-GFP was present in the cell body but absent in the neurites (Fig. 2B and E). After 2 h of DOX treatment, FMRP-GFP was present both in the cell body and in the neurites, and especially in the neurites FMRP-GFP appeared as granules (arrows, Fig. 2C and F).

As a control for the physiological relevance of the results described above, the endogenous FMRP expression in both PC12 cells (not transfected; Fig. 2G) and primary cultures of mouse (wt) hippocampal neurons (Fig. 2H) was studied with monoclonal antibodies to FMRP. Endogenous FMRP showed a similar labeling pattern as that of FMRP-GFP in PC12/FMR7 cells after DOX treatment.

From these steady-state images no conclusions could be made as to whether the appearance of FMRP-GFP-positive granules within the neurites was the result of transport from the cell body or of local translation in the neurites. Therefore, the expression pattern was studied again in a time series but now in the presence of cycloheximide, an inhibitor of mRNA translation. First PC12/FMR7 cells were exposed to NGF for 72 h followed by DOX induction for 30 min. Subsequently, the DOX induction was continued for another 2 h but now in the presence of cycloheximide. Figures 2I to K illustrate the results of this experiment. After only 30 min of DOX induction, FMRP-GFP was present solely in the cell body (Fig. 2I) as shown above (Fig. 2E). Figures 2J and K show the presence of FMRP-GFP in granules located in the neurites (arrows) in cells after 2.5 h of DOX induction in the absence (Fig. 2J) and presence (Fig. 2K) of cycloheximide. No differences in expression pattern could be observed between cells that were treated with and without cycloheximide.

Time-lapse fluorescent microscopy. Time-lapse microscopy was performed to study the cellular movement of FMRP-GFP-positive granules in PC12/FMR7 cells, with special emphasis on the trafficking into neurites. Figures 3 and 4 correspond to time-lapse sequences 1 and 2, respectively (both time-lapse versions are available online at www.eur.nl./fgg/ch1/pc12). The first time-lapse sequence shows the movement of FMRP-GFP granules in a time-lapse study of frames every 5 s for 500 s. FMRP-GFP granules are continually moving out of the swelling along the neurite (Fig. 3A, square 2) into distal neurites (anterograde transport).

Quantification of the intensity of these fluorescent granules and a graphic presentation are given in Fig. 3B for different areas within the cell over time. The overall intensity in the cell body remains the same during the total recorded time period

(Fig. 3B, square 3). In contrast, the intensity in the swelling along the neurite varies over time, that is, approximately every 3 min we could observe a cycle in which the fluorescent intensity slowly decreased and subsequently slowly increased. The intensity in the growth cone (Fig. 3B, rectangle 1) gradually increases over time. In this time-lapse microscopy experiment we observed that the transport rate of the granules was too high for accurate observation. Therefore, the movement of FMRP-GFP granules was studied between the swelling along the neurite and the growth cone within this same cell at shorter time intervals (sequence 2, one frame per second for 300 s). The movement of granules could be categorized as unidirectional anterograde and oscillatory. Figure 4 shows a selection of consecutive time-lapse frames (every 2 s) and illustrates the bidirectional (anterograde and retrograde) movement of an FMRP-GFP granule (Fig. 4, arrow). The movement of the granules was not linear but rather saltatory, and not all granules were moving continuously. In addition, the average velocity of the FMRP-GFP particles has been determined by analyzing the motility characteristics of 25 different particles. Thirty distances were measured, and an average speed of 0.19 ± 0.03 (standard error of the mean) μm/s was calculated with a maximum observed speed of 0.71 μm/s.

Colocalization experiments and drug treatments. Colocalization experiments were performed to further characterize the FMRP-GFP granules by using specific antibodies to proteins known to interact with FMRP and proteins already known to be present in RNP particles. EtBr was used to label total cellular RNA. PC12/FMR7 cells were exposed to NGF for 72 h and subsequently treated for 24 h with both NGF and DOX. Labeling with EtBr revealed an intense RNA signal in the cell body and to a lesser extent in the neurites. In neurites, EtBr staining overlaps with the FMRP-GFP granules (Fig. 5A to C). We found a strong colocalization of FMRP-GFP granules and P0, a 60S ribosomal component (Fig. 5D to F). Studies of colocalization between FMRP-GFP and kinesin (heavy chains), a microtubule-based motor molecule, demonstrated in neurites an overlap between the two proteins (Fig. 5G to I). Next, the codistribution of FMRP-GFP and FXR1P, a fragile X-related protein and a known interactor with FMRP, was studied, and again a clear colocalization could be observed (Fig. 5J to L). The colocalization of FMRP-GFP with these proteins and RNA was observed in both the bigger and smaller granules. No colocalization with FMRP-GFP was observed with nucleolin, MAP2, MAP1B, synaptophysin, neurofilament (160 kDa), and dynein (C_{18}, motor protein) (data not shown).

In neurons, both microtubules and/or microfilaments (e.g., actin) are involved in the transport of RNP particles into neurites. Cytoskeleton-disrupting drugs were used to investigate which transport system was responsible for movement of the FMRP-GFP granules. These drugs were injected into the medium after 30 min of treatment of the cells with DOX, to

FIG. 5. PC12/FMR7 cells (after 24 h of DOX treatment) double labeled on the one hand for FMRP-GFP (A, D, G, and J) and on the other hand for total RNA (B), ribosomal subunits (P0) (E), kinesin heavy chain (H), and FXR1P (K). For each individual colocalization experiment we have included an image that merges both separate images (green and red). Colocalization results in a yellow color (C, F, I, and L). Photographs show part of a neurite and growth cone with two populations of granules (larger and smaller). Both types of granules show colocalization. Magnifications: A to I, ×2,880; J to L, ×1,600.
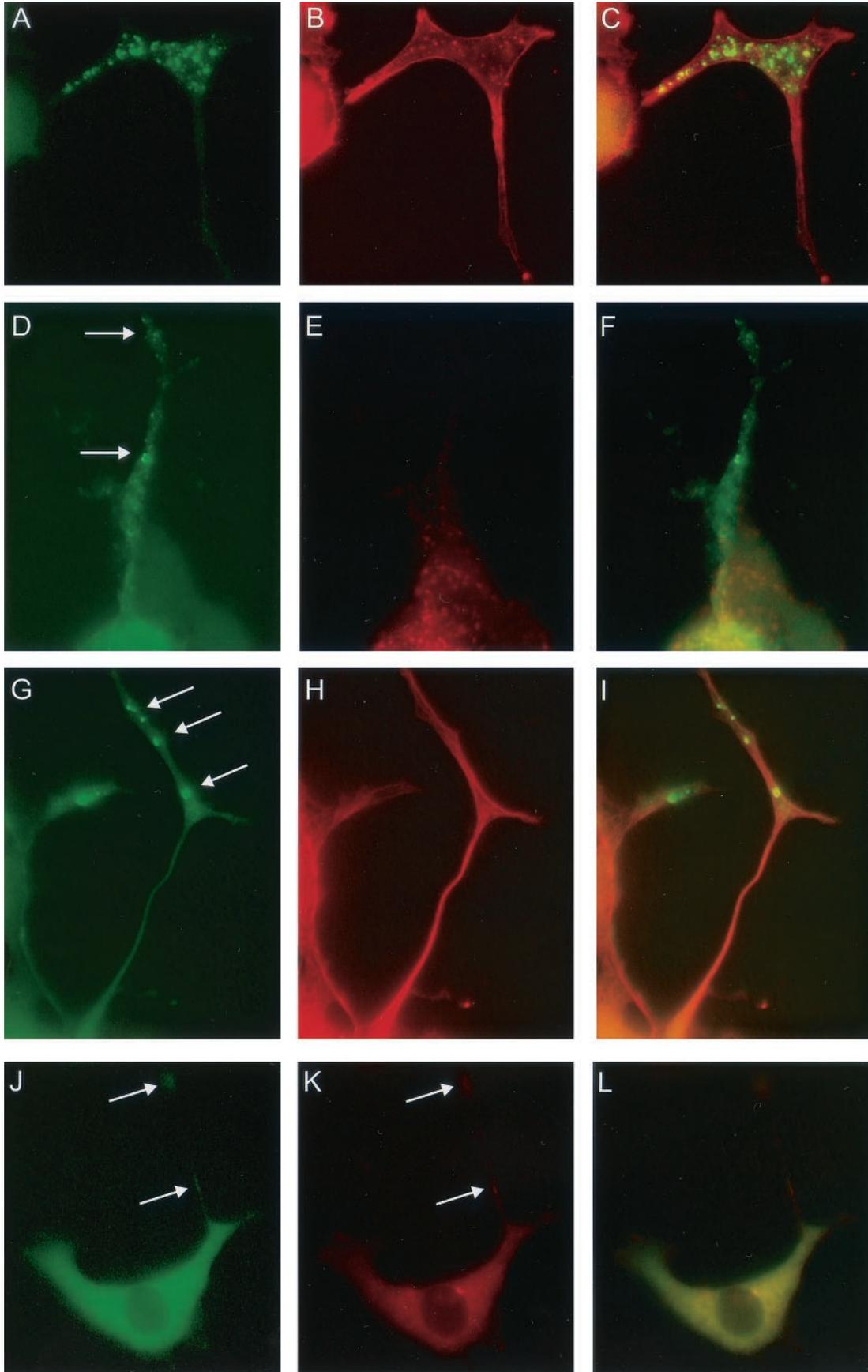
ensure that FMRP-GFP granules were not yet present in neurites, for a total period of 2 h. Exposure of the cells to cytochalasin D, which disrupts the actin filaments (12), had no effect on the distribution of FMRP-GFP granules in the neurites. Figures 6A to 6C illustrate the localization of F-actin (red) and FMRP-GFP (green) without exposure to cytochalasin D. Within the neurite a clear intact actin network could be observed, especially in the growth cone, together with nonoverlapping FMRP-GFP granules that had reached the growth cone in the 2-h period. However, after exposure to cytochalasin D (Fig. 6D to F) the actin network was destroyed (Fig. 6E), but FMRP-GFP granules were normally localized within the neurites (Fig. 6D, arrows). In contrast, treatment of PC12/FMR7 cells with nocodazole, which depolymerizes microtubules (41), resulted in the absence of FMRP-GFP granules in the neurites. Without nocodazole treatment, FMRP-GFP granules were transported into the neurites (Fig. 6G, arrows) in the total 2.5-h time period of DOX induction, and the cells showed a clear nonoverlapping microtubule network staining (Fig. 6H). Interestingly, after nocodazole treatment FMRP-GFP granules were not transported into the neurites (Fig. 6J), which showed only a very faint staining for microtubules (Fig. 6K, arrows).

DISCUSSION

Localized mRNAs within mammalian cells provide the basis for a spatial distribution of functions in a cell, and translocation of specific mRNAs to specific cellular compartments has been reported for many cell types. A number of mRNAs have been reported to be selectively targeted to dendrites of neurons, and these include for instance mRNAs for MAP2, Arc, CaMKIIα, and glutamate receptors (7, 16, 22, 29). There is evidence that for dendrites an active sorting mechanism is involved. Certain neuronal mRNAs like MAP2 and CaMKIIα contain dendritic targeting signals in their 3' untranslated regions (5, 30). Several potential mRNA binding proteins have been identified which recognize these targeting sequences. These proteins include hnRNP A2 and Staufen (18, 36). It has been postulated that FMRP might perform a similar function in transporting mRNAs containing a G-quartet structure and in regulating their translation at the synapse (13). Therefore, the distribution and transport of FMRP were studied in a neuronal cell model system.

The neuroendocrine PC12 cell line originates from a rat pheochromocytoma and is commonly used as a model system for neuronal differentiation (17). Upon exposure to NGF, PC12 cells develop neurites but no axons. Furthermore, differentiated cells contain synapse-like vesicles, including synapse-like vesicle membrane proteins (40). Here we describe the development and characterization of an FMR1-EGFP stable transfected PC12 cell line with a Tet-On expression system, for tightly regulated expression of the FMR1-EGFP-encoding gene in response to DOX induction. Using Western blotting, we have shown that this cell line expresses a human full-length FMRP-GFP fusion protein after DOX induction. Although the Tet-On expression system is a high-level gene expression system, we have chosen a cell line with only a moderate expression rate of FMRP-GFP compared to endogenous rat Fmrp expression (data not shown). This enabled us to study the FMRP distribution and transport dynamics in living PC12 cells at almost physiological expression levels in neuronal processes during neuronal differentiation. Moreover, high FMRP expression levels in transiently transfected cells have been shown previously to have a toxic effect on the cells (10).

After DOX induction, FMRP-GFP appeared first in the cell body and later as granules (RNP particles) moving into the neurites. The size of the granules is not uniform, that is, two different populations of granules exist, larger and smaller granules. The bigger granules are better represented in the distal part of the neurites and growth cones. Ultimately, the granules accumulate in the swellings along the neurite and in the growth cone. Both time-lapse microscopy and steady-state localization studies in the presence of cycloheximide, an inhibitor of mRNA translation, demonstrate clearly the movement of FMRP-GFP-positive granules into the neurites. Interestingly, movement of the bigger granules was never observed; only the smaller granules moved into the neurites. This phenomenon and the fact that both types of granules showed colocalization with RNA, FXR1P, kinesin, and P0 suggest that the smaller ones fuse with each other to form the bigger ones.

Thus, at least part of the FMRP-GFP present in the growth cone is due to transport out of the cell body into the neurites. However, it is possible that local translation of FMR1-EGFP mRNAs occurs simultaneously. In synaptoneurosome preparations from rat cortex, both Fmr1 mRNA and Fmrp could be detected, and after mGluR1 stimulation a moderate increase of Fmrp expression within translational complexes was observed (42). These in vitro results suggest the occurrence of local Fmr1 mRNA translation in dendrites.

Quantification of the FMRP-GFP fluorescent labeling suggests a role for the swellings along the neurites as an intermediate in protein synthesis-transport between the cell body and growth cones. Frequently the swellings along the neurite branch off in several neurites. Perhaps the swellings along the neurite represent an intermediate compartment bridging the

FIG. 6. Shown are fluorescent images of PC12/FMR7 cells after 30 min of DOX induction followed by further treatment in (i) control medium (with DOX) for another 2 h (A, B, G, and H), (ii) medium supplemented with cytochalasin D for another 2 h (D and E), and (iii) medium supplemented with nocodazole for another 2 h (J and K). Colocalization experiments were performed with phalloidin conjugated with Texas red to visualize F-actin (B and E) and antibodies to tyrosine-tubulin to visualize microtubules (H and K). Treatment with cytochalasin D had no effect on the localization of FMRP-GFP granules in the neurites (compare green fluorescence of panels A and D), while the F-actin labeling in the neurites was completely abolished compared to that in untreated cells (compare red fluorescence of panels B and E). Treatment with nocodazole abolished the microtubules (compare red fluorescence of panels H and K; arrows in panel K point to a neurite with only very faint staining for tubulin), and FMRP-GFP granules were not transported into the neurites (compare green fluorescence of panels G and J, arrows). The two individual images (red and green) of each experiment were merged (C, F, I, and L) to visualize colocalization (yellow). FMRP-GFP granules in the neurites were not colocalized with either F-actin or tubulin. Magnifications: A to I, ×2,400; J to L, ×1,360.

long distance between the cell body and the growth cone. Our results show a decrease in intensity within the swelling every 1.5 min followed by a gradual increase of intensity in the growth cone. Surprisingly, the decrease within the swelling is succeeded by an increase within the same swelling during the next 1.5 min. This cycle of deflation and expansion repeats continuously over time. This increase may be due to either transport of newly synthesized FMRP-GFP molecules out of the cell body or local translation of FMR1 mRNAs. Whether local FMR1 mRNA translation can occur within the swellings along the neurite remains to be elucidated.

The FMRP-GFP-positive granules in the neurites displayed two types of movement: oscillatory (bidirectional) over short distances or unidirectional over larger distances in the direction of the growth cone (anterograde). The fact that only a small proportion of the granules actually move within a neurite has been reported elsewhere for SYTO14-, Staufen-GFP-, and CaMKIIα 3′-untranslated region–GFP-labeled granules too (23, 25, 32). The oscillatory movement of granules has been attributed to fine local adjustments within specific dendritic sites, i.e., clusters of synapses (32). We observed an average velocity of 0.19 μm/s, which is in line with earlier studies of granular mRNA transport kinetics that have produced rates of between 0.07 and 0.2 μm/s (1, 24, 31).

The presence of RNA, ribosomal subunits, kinesin heavy chain, and FXR1P in FMRP-GFP labeled granules further illustrates the macromolecular structure of the granules. The colocalization of FMRP-GFP labeled granules with RNA may reflect the presence of individual mRNAs as well as rRNA within the granules. Recent evidence suggests a role for these mRNP particles in dendritic mRNA transport and suggests that they may represent a mechanism in generating synaptic plasticity (21). Each individual protein within the mRNP particle may have a specific function (*cis*- and *trans*-acting factors) in recognition, transport, docking, stability, and translation efficiency of mRNAs. Ribosomal subunits may represent components of the translational machinery that are necessary at the same site as the translocated mRNA (24). Kinesin molecules are implied to play a role in mRNP particle transport along microtubules, especially in large cell types like neurons (4). Additionally, we demonstrate the microtubule-dependent transport of FMRP-GFP labeled granules into neurites by using the microtubule-depolymerizing drug nocodazole. Disruption of the microtubules prevents the transport of FMRP-GFP into neurites. In contrast, cytochalasin D, an actin-depolymerizing drug, has no influence on trafficking of the granules into the neurites. In the present study we showed that in vivo FMRP is also a component of the RNP particle. Thus, the present evidence shows that FMRP-GFP is recruited in RNA-containing granules representing RNP particles and transported into neurites along microtubules with an average speed of approximately 0.2 μm/s.

Synaptic plasticity may require local synthesis of proteins at the postsynaptic sites in response to synaptic activity. The local protein synthesis involves mRNAs already in place or trafficking of specific mRNAs induced by synaptic activity from the cell body into dendrites. Only a small subset of the total pool of mRNAs is transported into dendrites; thus, differential intracellular sorting of specific mRNAs is necessary to maintain the asymmetric distribution of mRNAs. The function of FMRP

within the mRNP particle might represent a role in this selective targeting of specific mRNAs. FMRP is an RNA binding protein that binds with high affinity to mRNAs via a G quartet (13, 33). Several mRNAs that contain a G quartet with a high affinity for FMRP were identified, and some were underrepresented in polysomes of lymphoblast cells from fragile X patients, including MAP1B and semaphorin (6). Only a minority (±4%) of the total mRNA pool contains such a G quartet; thus, the presence of a G quartet serves as a zip code for selective targeting of those mRNAs to dendrites. The cognitive deficits in fragile X syndrome are caused by the absence of FMRP in neurons and might be induced by misrouting and/or misregulation of specific G-quartet-containing mRNAs into dendrites, mRNAs which encode important neuronal proteins, including MAP1B and semaphorin. The new PC12 model system described in the present report might serve as an important tool to isolate and characterize the in vivo target mRNAs of FMRP in continuing studies using combined laser-dissection microscopy with reverse transcription-PCR and in situ hybridization techniques. Further identification of mRNA targets of FMRP, especially those mRNAs involved in normal synaptic activity, might provide knowledge about the role of FMRP in synaptic plasticity and memory storage.

REFERENCES

1. **Ainger, K., D. Avossa, F. Morgan, S. J. Hill, C. Barry, E. Barbarese, and J. H. Carson.** 1993. Transport and localization of exogenous myelin basic protein mRNA microinjected into oligodendrocytes. J. Cell Biol. **123:**431–441.
2. **Ashley, C., Jr., K. D. Wilkinson, D. Reines, and S. T. Warren.** 1993. FMR1 protein: conserved RNP family domains and selective RNA binding. Science **262:**563–568.
3. **Bakker, C. E., Y. de diego Otero, C. Bontekoe, P. Raghoe, T. Luteijn, A. T. Hoogeveen, B. A. Oostra, and R. Willemsen.** 2000. Immunocytochemical and biochemical characterization of FMRP, FXR1P, and FXR2P in the mouse. Exp. Cell Res. **258:**162–170.
4. **Bassell, G. J., Y. Oleynikov, and R. H. Singer.** 1999. The travels of mRNAs through all cells large and small. FASEB J. **13:**447–454.
5. **Blichenberg, A., B. Schwanke, M. Rehbein, C. C. Garner, D. Richter, and S. Kindler.** 1999. Identification of a cis-acting dendritic targeting element in MAP2 mRNAs. J. Neurosci. **19:**8818–8829.
6. **Brown, V., P. Jin, S. Ceman, J. C. Darnell, W. T. O'Donnell, S. A. Tenenbaum, X. Jin, Y. Feng, K. D. Wilkinson, J. D. Keene, R. B. Darnell, and S. T. Warren.** 2001. Microarray identification of FMRP-associated brain mRNAs and altered mRNA translational profiles in fragile X syndrome. Cell **107:**477–487.
7. **Burgin, K. E., M. N. Waxham, S. Rickling, S. A. Westgate, W. C. Mobley, and P. T. Kelly.** 1990. In situ hybridization histochemistry of Ca²⁺/calmodulin-dependent protein kinase in developing rat brain. J. Neurosci. **10:**1788–1798.
8. **Carson, J. H., S. Kwon, and E. Barbarese.** 1998. RNA trafficking in myelinating cells. Curr. Opin. Neurobiol. **8:**607–612.
9. **Castren, M., A. Haapasalo, B. A. Oostra, and E. Castren.** 2001. Subcellular localization of fragile X mental retardation protein with the I304N mutation in the RNA-binding domain in cultured hippocampal neurons. Cell. Mol. Neurobiol. **21:**29–38.
10. **Ceman, S., V. Brown, and S. T. Warren.** 1999. Isolation of an FMRP-

associated messenger ribonucleoprotein particle and identification of nucleolin and the fragile X-related proteins as components of the complex. Mol. Cell. Biol. **19:**7925–7932.

11. **Comery, T. A., J. B. Harris, P. J. Willems, B. A. Oostra, S. A. Irwin, I. J. Weiler, and W. T. Greenough.** 1997. Abnormal dendritic spines in fragile X knockout mice: maturation and pruning deficits. Proc. Natl. Acad. Sci. USA **94:**5401–5404.

12. **Cooper, J. A.** 1987. Effects of cytochalasin and phalloidin on actin. J. Cell Biol. **105:**1473–1478.

13. **Darnell, J. C., K. B. Jensen, P. Jin, V. Brown, S. T. Warren, and R. B. Darnell.** 2001. Fragile X mental retardation protein targets G quartet mRNAs important for neuronal function. Cell **107:**489–499.

14. **Devys, D., Y. Lutz, N. Rouyer, J. P. Bellocq, and J. L. Mandel.** 1993. The FMR-1 protein is cytoplasmic, most abundant in neurons and appears normal in carriers of a fragile X premutation. Nat. Genet. **4:**335–340.

15. **Feng, Y., C. A. Gutekunst, D. E. Eberhart, H. Yi, S. T. Warren, and S. M. Hersch.** 1997. Fragile X mental retardation protein: nucleocytoplasmic shuttling and association with somatodendritic ribosomes. J. Neurosci. **17:**1539–1547.

16. **Gazzaley, A. H., D. L. Benson, G. W. Huntley, and J. H. Morrison.** 1997. Differential subcellular regulation of NMDAR1 protein and mRNA in dendrites of dentate gyrus granule cells after perforant path transection. J. Neurosci. **17:**2006–2017.

17. **Greene, L. A., and A. S. Tischler.** 1976. Establishment of a noradrenergic clonal line of rat adrenal pheochromocytoma cells which respond to nerve growth factor. Proc. Natl. Acad. Sci. USA **73:**2424–2428.

18. **Hoek, K. S., G. J. Kidd, J. H. Carson, and R. Smith.** 1998. hnRNP A2 selectively binds the cytoplasmic transport sequence of myelin basic protein mRNA. Biochemistry **37:**7021–7029.

19. **Irwin, S. A., B. Patel, M. Idupulapati, J. B. Harris, R. A. Crisostomo, B. P. Larsen, F. Kooy, P. J. Willems, P. Cras, P. B. Kozlowski, R. A. Swain, I. J. Weiler, and W. T. Greenough.** 2001. Abnormal dendritic spine characteristics in the temporal and visual cortices of patients with fragile-X syndrome: a quantitative examination. Am. J. Med. Genet. **98:**161–167.

20. **Khandjian, E. W., B. Bardoni, F. Corbin, A. Sittler, S. Giroux, D. Heitz, S. Tremblay, C. Pinset, D. Montarras, F. Rousseau, and J. Mandel.** 1998. Novel isoforms of the fragile X related protein FXR1P are expressed during myogenesis. Hum. Mol. Genet. **7:**2121–2128.

21. **Kiebler, M. A., and L. DesGroseillers.** 2000. Molecular insights into mRNA transport and local translation in the mammalian nervous system. Neuron **25:**19–28.

22. **Kleiman, R., G. Banker, and O. Steward.** 1994. Development of subcellular mRNA compartmentation in hippocampal neurons in culture. J. Neurosci. **14:**1130–1140.

23. **Knowles, R. B., and K. S. Kosik.** 1997. Neurotrophin-3 signals redistribute RNA in neurons. Proc. Natl. Acad. Sci. USA **94:**14804–14808.

24. **Knowles, R. B., J. H. Sabry, M. E. Martone, T. J. Deerinck, M. H. Ellisman, G. J. Bassell, and K. S. Kosik.** 1996. Translocation of RNA granules in living neurons. J. Neurosci. **16:**7812–7820.

25. **Kohrmann, M., M. Luo, C. Kaether, L. DesGroseillers, C. G. Dotti, and M. A. Kiebler.** 1999. Microtubule-dependent recruitment of Staufen-green fluorescent protein into large RNA-containing granules and subsequent dendritic transport in living hippocampal neurons. Mol. Biol. Cell **10:**2945–2953.

26. **Kooy, R. F., R. Willemsen, and B. A. Oostra.** 2000. Fragile X syndrome at the turn of the century. Mol. Med. Today **6:**193–198.

27. **Laggerbauer, B., D. Ostareck, E. M. Keidel, A. Ostareck-Lederer, and U. Fischer.** 2001. Evidence that fragile X mental retardation protein is a negative regulator of translation. Hum. Mol. Genet. **10:**329–338.

28. **Li, Z., Y. Zhang, L. Ku, K. D. Wilkinson, S. T. Warren, and Y. Feng.** 2001. The fragile X mental retardation protein inhibits translation via interacting with mRNA. Nucleic Acids Res. **29:**2276–2283.

29. **Lyford, G. L., K. Yamagata, W. E. Kaufmann, C. A. Barnes, L. K. Sanders, N. G. Copeland, D. J. Gilbert, N. A. Jenkins, A. A. Lanahan, and P. F. Worley.** 1995. Arc, a growth factor and activity-regulated gene, encodes a novel cytoskeleton-associated protein that is enriched in neuronal dendrites. Neuron **14:**433–445.

30. **Mayford, M., D. Baranes, K. Podsypanina, and E. R. Kandel.** 1996. The 3′-untranslated region of CaMKII alpha is a *cis*-acting signal for the localization and translation of mRNA in dendrites. Proc. Natl. Acad. Sci. USA **93:**13250–13255.

31. **Muslimov, I. A., E. Santi, P. Homel, S. Perini, D. Higgins, and H. Tiedge.** 1997. RNA transport in dendrites: a *cis*-acting targeting element is contained within neuronal BC1 RNA. J. Neurosci. **17:**4722–4733.

32. **Rook, M. S., M. Lu, and K. S. Kosik.** 2000. CaMKIIalpha 3′ untranslated region-directed mRNA translocation in living neurons: visualization by GFP linkage. J. Neurosci. **20:**6385–6393.

33. **Schaeffer, C., B. Bardoni, J. L. Mandel, B. Ehresmann, C. Ehresmann, and H. Moine.** 2001. The fragile X mental retardation protein binds specifically to its mRNA via a purine quartet motif. EMBO J. **20:**4803–4813.

34. **Siomi, H., M. C. Siomi, R. L. Nussbaum, and G. Dreyfuss.** 1993. The protein product of the fragile X gene, FMR1, has characteristics of an RNA-binding protein. Cell **74:**291–298.

35. **Steward, O., and E. M. Schuman.** 2001. Protein synthesis at synaptic sites on dendrites. Annu. Rev. Neurosci. **24:**299–325.

36. **St. Johnston, D., D. Beuchle, and C. Nusslein-Volhard.** 1991. Staufen, a gene required to localize maternal RNAs in the Drosophila egg. Cell **66:**51–63.

37. **Sundell, C. L., and R. H. Singer.** 1991. Requirement of microfilaments in sorting of actin messenger RNA. Science **253:**1275–1277.

38. **Tamanini, F., R. Willemsen, L. van Unen, C. Bontekoe, H. Galjaard, B. A. Oostra, and A. T. Hoogeveen.** 1997. Differential expression of FMR1, FXR1 and FXR2 proteins in human brain and testis. Hum. Mol. Genet. **6:**1315–1322.

39. **Tang, S. J., D. Meulemans, L. Vazquez, N. Colaco, and E. Schuman.** 2001. A role for a rat homolog of staufen in the transport of RNA to neuronal dendrites. Neuron **32:**463–475.

40. **Tao-Cheng, J. H., A. Dosemeci, J. P. Bressler, M. W. Brightman, and D. L. Simpson.** 1995. Characterization of synaptic vesicles and related neuronal features in nerve growth factor and ras oncogene differentiated PC12 cells. J. Neurosci. Res. **42:**323–334.

41. **Vasquez, R. J., B. Howell, A. M. Yvon, P. Wadsworth, and L. Cassimeris.** 1997. Nanomolar concentrations of nocodazole alter microtubule dynamic instability in vivo and in vitro. Mol. Biol. Cell **8:**973–985.

42. **Weiler, I. J., S. A. Irwin, A. Y. Klintsova, C. M. Spencer, A. D. Brazelton, K. Miyashiro, T. A. Comery, B. Patel, J. Eberwine, and W. T. Greenough.** 1997. Fragile X mental retardation protein is translated near synapses in response to neurotransmitter activation. Proc. Natl. Acad. Sci. USA **94:**5395–5400.

43. **Willemsen, R., C. Bontekoe, F. Tamanini, H. Galjaard, A. T. Hoogeveen, and B. A. Oostra.** 1996. Association of FMRP with ribosomal precursor particles in the nucleolus. Biochem. Biophys. Res. Commun. **225:**27–33.